

Interface Acoustic Waves Properties in Some Common Crystal Cuts

Serge Camou, Vincent Laude, *Member, IEEE*, Thomas Pastureaud, and Sylvain Ballandras

Abstract—Interface acoustic waves (IAWs), also termed boundary waves, propagate at the interface between two solids. We present two IAW numerical analysis tools, inspired from well established surface acoustic wave (SAW) methods. First, the interface effective permittivity is derived for arbitrary piezoelectric solids and is used to estimate some basic parameters of IAWs. The harmonic admittance for an interface excitation is then derived from the interface effective permittivity, in much the same way the harmonic admittance for surface excitation is obtained from the (surface) effective permittivity. The finite electrode thickness is neglected in this problem analysis. The harmonic admittance is used to model propagation in case an infinite periodic interdigital transducer is located at the interface. Simulation results are commented upon for some usual piezoelectric material cuts and outline a modal selection specific to IAWs as compared with SAWs. The temperature dependence of the resonance frequency is also estimated.

I. INTRODUCTION

WITH the fast evolution of passive high-frequency filtering requirements, typically driven by mobile telephony, much effort has been devoted to the improvement of classical single-crystal surface acoustic wave (SAW) solutions. Among possible new devices, the use of interface acoustic waves (IAWs) [1] in place of SAWs has been proposed by some authors. An IAW, also termed a boundary wave, propagates at the interface between two solids, and the special case that at least one of the solids is piezoelectric has received much attention [2]–[12]. Ideally, if the IAW is perfectly guided by the interface, its amplitudes are expected to be evanescent or inhomogeneous in both materials. In case this guiding is not perfect, bulk waves can be radiated in both materials, leading to propagation losses. Significantly, one of the most cited advantages of IAW devices as opposed to SAW devices is the natural protection of the excitation interface, which is isolated from, and hence insensitive to, external perturbations, such as dust or wetness. This should lead to a simplification of packaging requirements, especially at high frequencies.

The existence of IAWs was first predicted by Stoneley [1] in the context of geology but for isotropic materials

only. The polarization of the Stoneley wave is in the sagittal plane, and its existence depends on the relative values of the material constants of the two solids. Maerfeld and Tournois [2] have shown that an IAW of transverse type exists at the interface of two piezoelectric crystals in class 6 mm, or one of these and an isotropic material, and that such an interface wave can be electrically excited. The existence of this wave is also restricted depending on the relative values of the material constants of the two solids.

Although several studies [5], [7], [9], [10], [12] have investigated IAWs with materials escaping the cases described above, i.e., isotropic solids and piezoelectric crystals in class 6 mm, we are neither aware of a general existence condition for interface acoustic waves nor of general prediction methods for their properties. In this work, we extend two classical methods of SAW analysis to the determination of IAW characteristics. First, the interface effective permittivity is derived for arbitrary piezoelectric solids and is used to estimate some basic parameters of IAW propagating at an ideally metallized (infinitely thin metal layer) interface or at a free interface. The polarization of the IAW is obtained at the same time. It is worthwhile noting that the attenuation of the IAW is explicitly taken into account and estimated; we are thus able to identify and characterize leaky IAWs. Second, the harmonic admittance at an interface is derived from the interface effective permittivity in much the same way the harmonic admittance at a surface is based on the (surface) effective permittivity in the celebrated Blötekjær method [13], [14]. The harmonic admittance is used to model propagation in case an infinite periodic interdigital transducer is located at the interface. The thickness of the interdigital transducer and the influence of its mass are neglected in this approach.

Simulation results are commented upon for some usual piezoelectric material cuts and outline a modal selection specific to IAWs as compared with SAWs. Following Danicki *et al.* [10], we have chosen to consider two identical piezoelectric half-spaces, for instance, obtained by separating some substrate in two parts, which are then bonded together after some surface preparation to include an interdigital transducer (IDT) at the interface for the excitation of the IAW. This special configuration has the advantage that an IAW is always found to exist in the simulations, although it usually suffers attenuation. Interestingly, the temperature dependence of the resonance frequency can also be estimated in this case by adapting the widespread Campbell and Jones approach [15].

Three usual piezoelectric cuts are investigated in this work, i.e., 42.75°YX quartz, 36°YX lithium tantalate

Manuscript received May 16, 2002; accepted February 28, 2003.

The authors are with the Laboratoire de Physique et de Métrologie des Oscillateurs, CNRS UPR 3203, associé à l'Université de Franche-Comté, 32 avenue de l'Observatoire, F-25044 Besançon, France (e-mail: vincent.laude@lpmo.edu).

S. Camou is now with the LIMMS/CNRS-IIS, University of Tokyo, Tokyo, Japan.

Th. Pastureaud is now with Thales Microsonics, Sophia Antipolis, France.

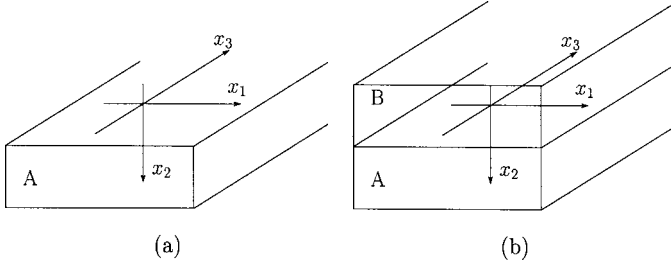


Fig. 1. Definition of axes for (a) surface acoustic waves on a substrate A and (b) interface acoustic waves at the interface between materials A and B. Propagation is along axis x_1 .

(LiTaO₃), and 64°YX lithium niobate (LiNbO₃). These cuts have in no way been chosen to optimize IAW operation but rather to illustrate IAW features different from or similar to well-known SAW cuts.

II. EFFECTIVE INTERFACE PERMITTIVITY

In this section, the propagation of IAWs is investigated at a free or metallized interface. With such homogeneous boundary conditions, plane wave solutions can be obtained naturally. The problem of the propagation of electroacoustic plane waves inside a piezoelectric medium has long been solved, and many equivalent formulations are available. Our derivation is based on the popular Fahmy and Adler solution [16], which is summarized below.

The geometry of the problem is depicted in Fig. 1, in which the axes are also defined. Propagation of plane waves at frequency f is considered along the x_1 axis, with slowness s_1 , at the interface between materials A and B. At least one of these materials is assumed piezoelectric and the other possibly dielectric. Assuming plane wave propagation in the structure, the distribution of the electromechanical fields inside both media is fully described [16], [17] using the eight-component state vector $\mathbf{h} = (u_1, u_2, u_3, \phi, T_{21}, T_{22}, T_{23}, D_2)^t$ where the u_i are the mechanical displacements, ϕ is the electrical potential, T_{ij} is the stress tensor, and D_2 is the normal electrical displacement. This state vector is obtained inside each medium as a superposition of eight partial modes, characterized by their eigenvalues $s_2^{(\alpha)}$ and their associated eigenvectors, where α is either A or B. The eigenvalues $s_2^{(\alpha)}$ only depend on the material constants of medium α , and on the slowness s_1 . Denoting $F^{(\alpha)}$ the 8×8 matrix of the vertically arranged eigenvectors, this superposition reads

$$\mathbf{h}(x_2) = F^{(\alpha)} \Delta^{(\alpha)}(x_2) \mathbf{a}^{(\alpha)} \exp(2j\pi f(t - s_1 x_1)), \quad (1)$$

where the dependence of the fields along axis x_2 is contained in the 8×8 diagonal matrix $\Delta^{(\alpha)}$ whose elements are

$$\Delta_{ii}^{(\alpha)}(x_2) = \exp(-2j\pi f s_{2,i}^{(\alpha)} x_2). \quad (2)$$

TABLE I

PARTIAL MODES CLASSIFICATION RULE. $P_{2,i}$ IS THE COMPONENT ALONG AXIS x_2 OF THE POYNTING VECTOR ASSOCIATED WITH PARTIAL MODE NUMBER i .

Partial modes	Propagative	Inhomogeneous
Reflected	$\Im(s_{2,i}) = 0$ and $P_{2,i} > 0$	$\Im(s_{2,i}) < 0$
Incident	$\Im(s_{2,i}) = 0$ and $P_{2,i} < 0$	$\Im(s_{2,i}) > 0$

$\mathbf{a}^{(\alpha)}$ is the vector of the eight amplitudes of the partial waves, whose values are obtained when the boundary conditions are specified.

It is well known that the eight partial modes in each medium can be classified in two groups of four partial modes, which are termed either reflected or incident, according to the convention summarized by Table I. In order to represent a valid physical solution, the superposition in (1) must not include incident partial modes in medium A or reflected partial modes in medium B. The superposition in (1) then involves only four partial mode amplitudes in each medium. Solving the boundary value problem at the interface will determine the remaining eight independent partial mode amplitudes.

In the formulation of Fahmy and Adler, the eight components of the state vector have been explicitly chosen such that they are continuous across any free interface inside a multilayer. In the case of the excitation of interface waves, a spatial charge density q must be allowed for at the interface, resulting in a discontinuity of the normal electrical displacement, while all seven other components are continuous. These considerations lead to the equation

$$F^{(A)} \mathbf{a}^{(A)} - F^{(B)} \mathbf{a}^{(B)} = q \begin{pmatrix} 0 \\ \vdots \\ 0 \\ 1 \end{pmatrix}, \quad (3)$$

where use has been made of the fact that $\Delta^{(\alpha)}(0)$ is the identity matrix, and matrices $F^{(\alpha)}$ have been restricted to their useful 8×4 elements. Eq. (3) can easily be solved by defining an eight-component unknown vector $\mathbf{a} = (\mathbf{a}^{(A)}, \mathbf{a}^{(B)})$, and an 8×8 matrix $F = (F^{(A)} | -F^{(B)})$. Its solution reads

$$\mathbf{a} = q F^{-1} \begin{pmatrix} 0 \\ \vdots \\ 0 \\ 1 \end{pmatrix}. \quad (4)$$

Once the vector \mathbf{a} is determined, it is easy to obtain the value of the state vector \mathbf{h} at the interface from (1) and hence the potential and the displacements. The displacements describe the polarization of the interface wave.

A direct relationship between the interface charge density and the interface potential has just been obtained. To characterize the electrical excitation of IAWs, it will be useful to define an effective interface permittivity similar

to the effective surface permittivity first introduced by Ingbrigtsen [18] for SAWs. This is defined as the ratio of the interface charge density to the tangential electrical field in the x_1 direction or

$$\varepsilon_{\text{eff}} = \frac{1}{j\varepsilon_0|s_1|} \frac{q}{\phi}. \quad (5)$$

Just as the effective surface permittivity contains information on all acoustic waves that are piezoelectrically coupled at the surface of a substrate, the effective interface permittivity contains information on all acoustic waves that are piezoelectrically coupled at an interface, including IAWs. Many authors have discussed how the effective permittivity can be used to estimate some basic parameters of SAWs [19], [20]; most of these methods can certainly be employed with little alteration in the case of IAWs, and in Section IV, we give several examples of IAW characterization using the effective interface permittivity. A pole in the effective interface permittivity is the signature of an IAW propagating along a metallized interface, with a finite interface charge density but a zero interface potential; these conditions are equivalent to those of a metallized surface in the case of a SAW. A zero in the effective interface permittivity is the signature of an IAW propagating along a free interface, with a zero interface charge density but a finite interface potential; these conditions are equivalent to those of a free surface in the case of a SAW. This observation raises, however, the question of the nature of the IAW guided by a free interface, especially in the case that both media are identical. Indeed, it might seem obvious physically that only bulk acoustic waves would propagate in this case and that these would not be guided at all by the interface, which is paradoxical. The solution to this paradox is that the IAW propagating along a free interface is not necessarily composed of homogenous partial modes (bulk waves) only but must include evanescent or inhomogeneous partial modes, although such a decomposition is usually not considered for bulk media. Furthermore, Danicki *et al.* [10] have established the need for a conductive layer at the interface of two identical half-spaces for perfect guiding of the IAW. Hence, in this case, the IAW at the free interface necessarily suffers attenuation.

The sensitivity of IAW devices to temperature can be estimated following the method of Campbell and Jones [15], by replacing the effective surface permittivity in the original approach by the effective interface permittivity, although this is only applicable in theory if both materials are identical, as argued below. The relative shift of the synchronism frequency generated by thermal perturbations can be related to the velocity shift and the thermal expansion of the material through

$$\frac{\Delta f}{f_o}(\Delta T) = \frac{\Delta v}{v_o}(\Delta T) - \frac{\Delta l}{l_o}(\Delta T). \quad (6)$$

The thermal expansion $l(T)$ in the direction of propagation is evaluated from the thermal expansion coefficients of the materials. If both materials are identical, the whole structure behaves thermally as a single bulk material, provided

the stress caused by bonding and the finite thickness of the metallic film can be neglected. If this is not true or if the materials are different, mechanical constraints in the vicinity of the interface depend strongly on the nature of the interface, and no attempt is made in this work to solve this problem. The variation of the velocity v with the temperature is evaluated from the thermal expansion coefficients of the material constants and also from the thermal expansion coefficients of the material to describe the variation of the mass density. It is well known that the relative frequency variation with temperature of elastic wave devices shows, in most cases, a parabolic shape. A fit of this curve to a parabolic model gives an estimate for the first-order temperature coefficient of frequency (TCF1) and of the second-order temperature coefficient of frequency.

III. HARMONIC ADMITTANCE FOR INTERFACE WAVES

The plane wave solutions obtained in the previous section are useful only to characterize IAW propagation along an homogeneous interface. As almost all SAW devices use IDTs on the surface to generate and detect surface acoustic waves, it has long been clear that the IDT itself influences the SAW characteristics. Among the many methods that have been proposed, the celebrated Blötekjær approach [13], [14] is a very elegant and fast way of obtaining the harmonic admittance of an infinite periodic IDT, based on the effective surface permittivity, but however fails to take into account the influence of the finite electrode thickness. Several improvements have been proposed to incorporate this effect in the harmonic admittance computation, e.g., [21]–[24]. All these methods rely on using finite element analysis inside the electrodes and relating the results obtained to a plane wave solution inside the substrate. Such a procedure is not directly transposable to the case of interface waves, because there are two surrounding media and, hence, two connecting interfaces between electrodes and media. In this work, we will then neglect the influence of the finite electrode thickness in the case of interface waves and leave it to future research. We next discuss how the Blötekjær method can be amended to include the case of interface waves.

The considered geometry is depicted in Fig. 2. An infinite periodic IDT, with a period p , is assumed to be present at the interface. The IDT is modeled as an infinitely thin perfect metallic pattern. A potential sequence is imposed to the fingers, according to the harmonic excitation rule

$$V_n = V_0 \exp(-2j\pi\gamma n), \quad (7)$$

where n is the index of the finger and γ is a parameter. The case $\gamma = 1/2$ corresponds to the $\pm V_0$ potential alternation characteristic of most practical IDTs. The Blötekjær method in the context of SAW makes use of the surface effective permittivity. It is remarkable and straightforward that the whole original derivation can be used unchanged in the case of interface waves, by replacing the surface

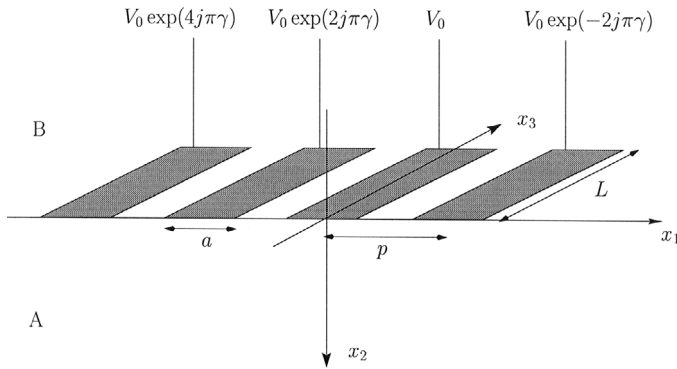


Fig. 2. Definitions relative to the harmonic admittance of an infinite periodic interdigital transducer (IDT) at the interface between two media.

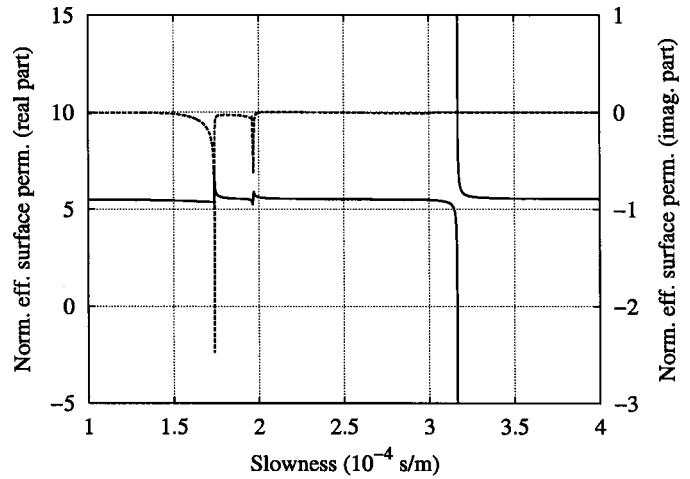
effective permittivity with the interface effective permittivity. The harmonic admittance $Y(\gamma)$, the ratio of the harmonic interface charge density to the harmonic potential, is then easily obtained. A number of useful tools have been constructed upon the harmonic admittance to obtain the propagation characteristics of surface waves [19], [25], [26] in a periodic IDT; they can be used unchanged for interface waves. We use the method described by Ventura *et al.* [25]: IAW parameters are obtained from a fit to a mixed matrix model and include the phase velocity, the attenuation per IDT period, the reflection coefficient per IDT period, and the electromechanical coupling.

IV. RESULTS

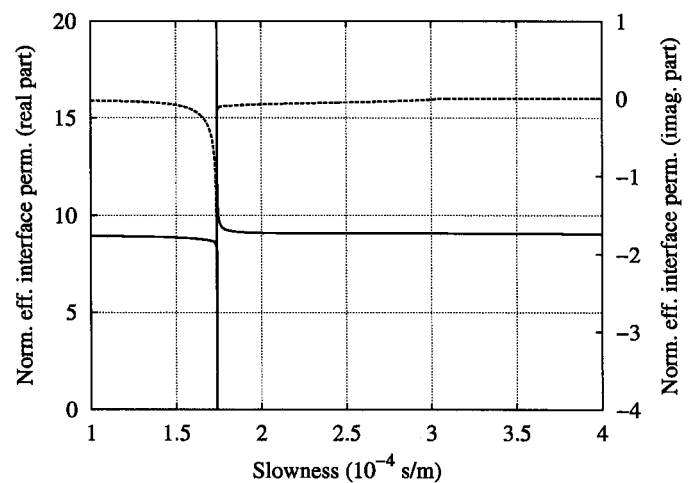
The effective interface permittivity and harmonic admittance tools introduced in Section II and III, respectively, are now used to compare interface acoustic waves with their surface acoustic wave counterparts in three common piezoelectric cuts. Materials A and B in Fig. 1(b) are then taken to be identical in the following. The considered cuts are 42.75°YX quartz, the so-called (ST, X) cut, which is well known to support a Rayleigh SAW with a zero TCF1 but a rather small electromechanical coupling, 36°YX lithium tantalate, which presents a widely used pseudo surface acoustic wave (PSAW) or leaky-SAW with a moderate TCF1 and a rather large electromechanical coupling, and 64°YX lithium niobate, which presents a PSAW with a large TCF1 and a large electromechanical coupling.

Fig. 3 to 5 show the effective surface and interface permittivities for 42.75°YX quartz, 36°YX lithium tantalate, and 64°YX lithium niobate, respectively, while Table II displays the wave parameters estimated from the effective permittivity and the harmonic admittance for these material cuts. In addition, Fig. 6 shows the modal structure of the IAWs listed in Table II. The normalized displacements are plotted as a function of the product fx_2 and illustrate the trapping of the modes at the interface.

In the case of 42.75°YX quartz, it is seen that the surface effective permittivity has a pole at a velocity of



(a)

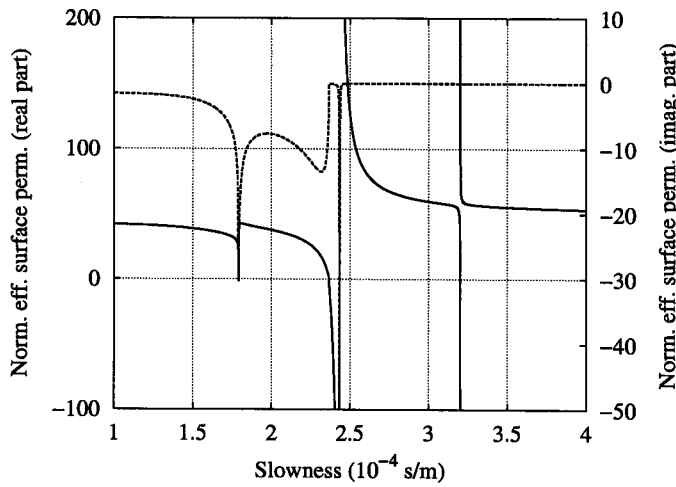


(b)

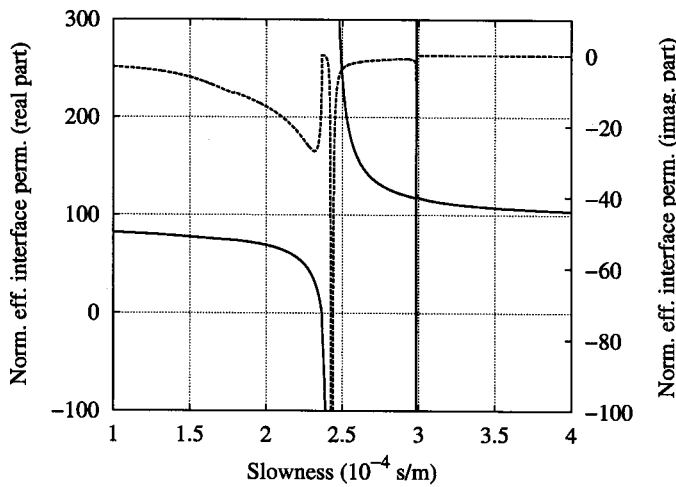
Fig. 3. 42.75°YX quartz (a) effective surface permittivity and (b) effective interface permittivity.

3158 m/s (slowness of $3.166 \cdot 10^{-4}$ s/m), caused by the Rayleigh SAW. The interface effective permittivity is in comparison very smooth, with a pole at a velocity of 5747 m/s (slowness of $1.740 \cdot 10^{-4}$ s/m), indicating that the longitudinal bulk acoustic wave has been converted to an interface wave. An examination of the polarization of this IAW indeed shows it is a longitudinal wave. A small attenuation is found, indicating that the IAW is not perfectly guided by the interface. Furthermore, in Fig. 6(a), the mode is only weakly guided by the interface, since the displacements converge slowly to zero far from the interface. A bad point with this IAW is, however, its very small coupling (K^2 value), which will make it difficult to use in practice. In addition, the zero TCF1 value for the SAW is lost for the IAW.

The cases of 36°YX lithium tantalate and 64°YX lithium niobate are rather similar, which is attributed to their identical 3-*m*-trigonal point group, as opposed to the 32-trigonal point group of quartz. Their effective surface



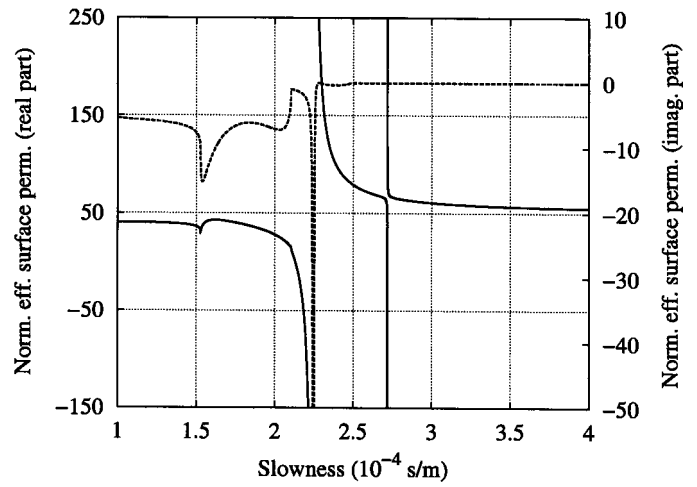
(a)



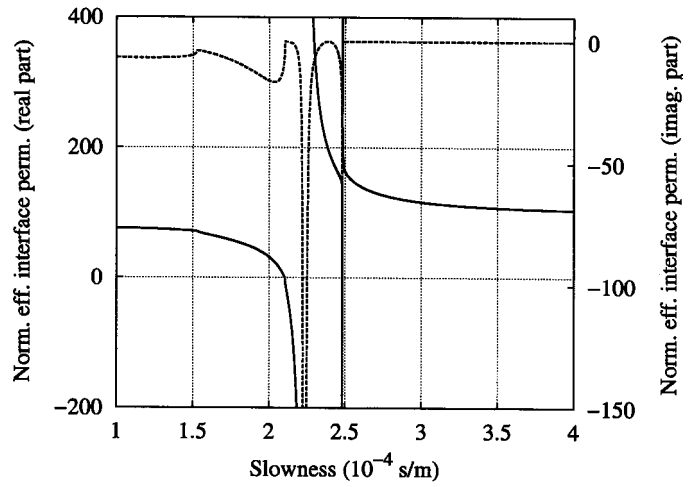
(b)

Fig. 4. 36°YX lithium tantalate (a) effective surface permittivity and (b) effective interface permittivity.

permittivities have a pole caused by a true SAW, i.e., with no attenuation, with a small coupling; the true SAW is generally not used with these cuts. The true SAW has a velocity of 3124 m/s (slowness of $3.201 \cdot 10^{-4}$ s/m) for 36°YX lithium tantalate and a velocity of 3679 m/s (slowness of $2.718 \cdot 10^{-4}$ s/m) for 64°YX lithium niobate. The effective surface permittivity also has a pseudopole caused by a PSAW, with limited attenuation and large coupling, which is often used in modern devices. The PSAW has a velocity of 4109 m/s (slowness of $2.488 \cdot 10^{-4}$ s/m) for 36°YX lithium tantalate and a velocity of 4451 m/s (slowness of $2.247 \cdot 10^{-4}$ s/m) for 64°YX lithium niobate. Note that these figures are given for a metallized surface. The effective interface permittivity shows basically the same features as the effective surface permittivity. A weakly coupled IAW with small attenuation appears at a velocity of 3351 m/s (slowness of $2.984 \cdot 10^{-4}$ s/m) for 36°YX lithium tantalate and a velocity of 4031 m/s (slowness of $2.481 \cdot 10^{-4}$ s/m) for 64°YX lithium niobate, which is almost ex-



(a)



(b)

Fig. 5. 64°YX lithium niobate (a) effective surface permittivity and (b) effective interface permittivity.

actly the velocity of the slow shear bulk acoustic wave in these materials. A strongly coupled IAW with rather strong attenuation appears also at a velocity of 4113 m/s (slowness of $2.431 \cdot 10^{-4}$ s/m) for 36°YX lithium tantalate and a velocity of 4475 m/s (slowness of $2.235 \cdot 10^{-4}$ s/m) for 64°YX lithium niobate. These leaky-IAWs are very close to the corresponding PSAW, having almost the same polarization, velocity, coupling, reflection coefficient per period, and TCF1. They have, however, a much larger attenuation. From Fig. 6(b) and 6(c), it can be observed that they are efficiently guided by the interface.

From these results, it may be inferred that interface waves are in practice not as useful as surface waves, mostly because their attenuation is found to be larger. However, it must be emphasized that the cuts considered in this work are among the most interesting cuts for SAW applications and the result of years of selection. There is no reason *a priori* that they would be equally successful as IAW cuts. It appears reasonable that an exhaustive search for good

TABLE II

COMPARISON OF SAWS AND IAWs FOR SOME PIEZOELECTRIC MATERIALS. POLARIZATION TRIPLETS ($|u_1|^2, |u_2|^2, |u_3|^2$) ARE FOR THE NORMALIZED INTERFACE DISPLACEMENTS AT RESONANCE ($|u_1|^2 + |u_2|^2 + |u_3|^2 = 1$). THE REFLECTION COEFFICIENT PER PERIOD $|r|$ IS ESTIMATED FOR A METALLIZATION RATIO $a/p = 1/2$.

42.75° YX quartz		
	SAW	IAW
polarization	quasi-elliptic (0.301, 0.692, 0.007)	pure longitudinal (1, 0, 0)
velocity (m/s)	3157.9	5747.5
attenuation (mdB/λ)	0	0.08
coupling K^2 (%)	0.116	0.025
reflection coefficient per period (%)	0.04	0.007
TCF1 (ppm/K)	-0.6	-22.14
36° YX lithium tantalate		
	PSAW	IAW
polarization	quasi-transverse (0.004, 0.014, 0.982)	transverse (0, 0.008, 0.992)
velocity (m/s)	4109.2	4113.5
attenuation (mdB/λ)	0.26	11
coupling K^2 (%)	7.76	7.6
reflection coefficient per period (%)	2.16	2.18
TCF1 (ppm/K)	-27	-25
64° YX lithium niobate		
	PSAW	IAW
polarization	quasi-transverse (0.012, 0.123, 0.865)	transverse (0, 0.268, 0.732)
velocity (m/s)	4451.3	4475.1
attenuation (mdB/λ)	3.7	34
coupling K^2 (%)	11.3	14.4
reflection coefficient per period (%)	4.26	5.42
TCF1 (ppm/K)	-75	-75

IAW cuts should lead to much better results than those reported here. In addition, in this first approach, we have only considered associations of the same material, while the combination of two or more different materials should lead to even better solutions.

V. CONCLUSION

In this article, we have extended to IAWs two classical analysis methods used for SAWs, i.e., the effective permittivity and the harmonic admittance as computed using the Blötekjær approach. These analysis methods are widely used to characterize SAW material cuts and can be equally well used to characterize IAW material cuts. We have compared IAW and SAW properties with three classical cuts, i.e., 42.75° YX quartz, 36° YX lithium tantalate, and 64° YX lithium niobate. We have estimated the polarization, the velocity, the attenuation, the coupling, the reflection coefficient per period, and the first-order temperature coefficient of frequency (TCF1) of these waves. Although in the reported simulations we have only considered the case of the excitation of IAWs at an interface inside a single material, the methods employed are equally applicable to a combination of two different ma-

terials. They could be used in a systematic study of IAW cuts to perform an optimization of the choice of materials and their cuts.

ACKNOWLEDGMENTS

The authors acknowledge fruitful discussions with Pierre Tournois, Pascal Ventura, Marc Solal, M. Wilm, and A. Reinhardt.

REFERENCES

- [1] R. Stoneley, "Elastic waves at the surface of separation of two solids," *Proc. Roy. Soc.*, vol. A-106, pp. 416–428, 1924.
- [2] C. Maerfeld and P. Tournois, "Pure shear surface wave guided by the interface of two semi-infinite media," *Appl. Phys. Lett.*, vol. 19, pp. 117–118, 1971.
- [3] C. Lardat, J. P. Menot, and P. Tournois, "Delay lines using interfacial waves in solid-liquid solid structures," *IEEE Trans. Sonics Ultrason.*, vol. 22, no. 1, pp. 16–24, 1975.
- [4] D. A. Lee and D. M. Corbly, "Use of interface waves for non-destructive inspection," *IEEE Trans. Sonics Ultrason.*, vol. 24, no. 3, pp. 206–212, 1977.
- [5] K. Yamanouchi, K. Iwahashi, and K. Shibayama, "Piezoelectric acoustic boundary waves propagating along the interface between SiO₂ and LiTaO₃," *IEEE Trans. Sonics Ultrason.*, vol. 25, no. 6, pp. 384–389, 1978.

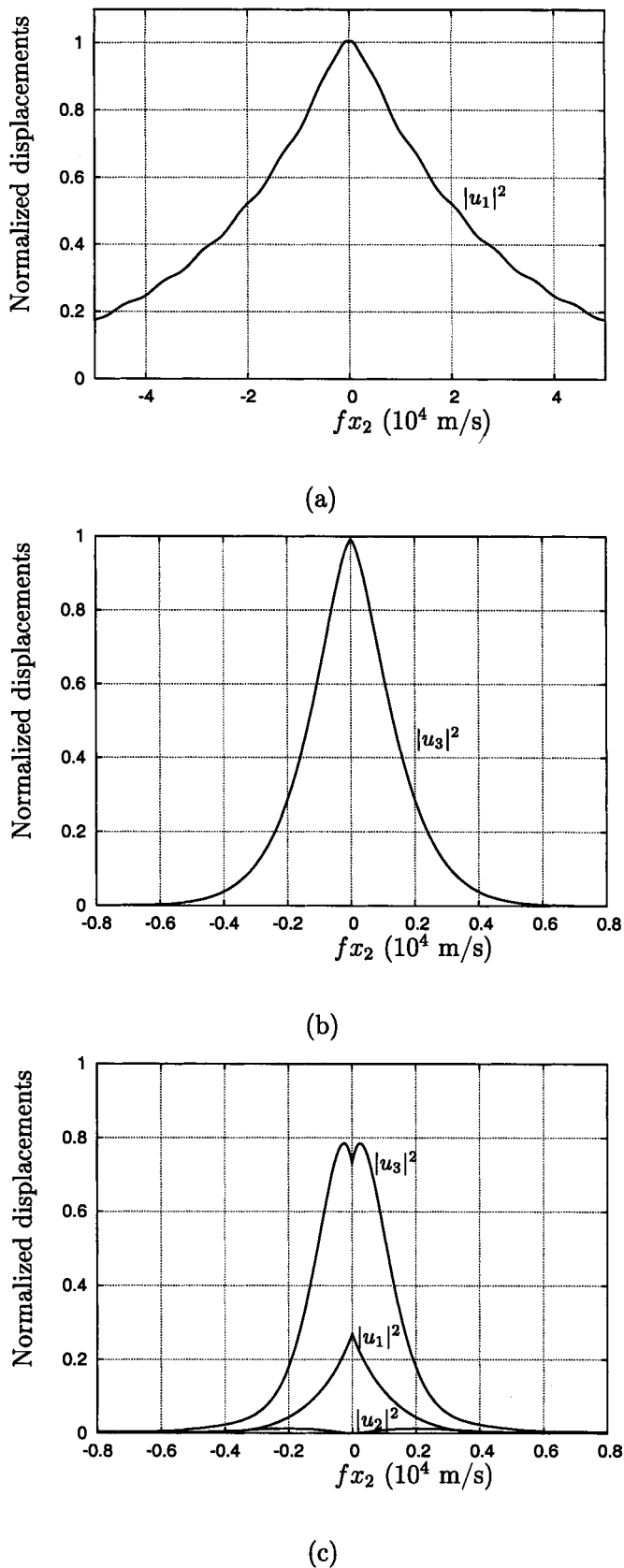


Fig. 6. Normalized displacements at resonance as a function of the product $f x_2$ for (a) 42.75° YX quartz, (b) 36° YX lithium tantalate, and (c) 64° YX lithium niobate. Note that $f x_2 = 0$ at the interface. The displacements are normalized such that $|u_1|^2 + |u_2|^2 + |u_3|^2 = 1$ at the interface.

- [6] R. O. Claus and C. H. Palmer, "Optical measurement of ultrasonic waves on interfaces between bonded solids," *IEEE Trans. Sonics Ultrason.*, vol. 27, no. 3, pp. 97–103, 1980.
- [7] T. Watanabe, T. Irino, and Y. Shimizu, "Zero slope temperature $\text{SiO}_2/\text{LiTaO}_3$ structure substrate for Stoneley waves," in *Proc. IEEE Ultrason. Symp.*, 1987, pp. 257–260.
- [8] T. Irino, Y. Suirosaki, and Y. Shimizu, "Propagation of boundary acoustic waves along a ZnO layer between two materials," *IEEE Trans. Ultrason., Ferroelect., Freq. Contr.*, vol. 35, no. 6, pp. 701–707, 1988.
- [9] T. Irino and Y. Shimizu, "Optimized Stoneley wave device by proper choice of glass overcoat," *IEEE Trans. Ultrason., Ferroelect., Freq. Contr.*, vol. 36, no. 2, pp. 159–167, 1989.
- [10] E. Danicki and W. Laprus, "Piezoelectric interfacial waves in langasite and dilithium tetraborate," in *Proc. IEEE Ultrason. Symp.*, 1995, pp. 1011–1014.
- [11] T. Yamashita, K. Hashimoto, and M. Yamaguchi, "Highly piezoelectric shear-horizontal-type boundary waves," *Jpn. J. Appl. Phys.*, vol. 36, no. 5B, pp. 3057–3059, 1997.
- [12] M. Yamaguchi, T. Yamashita, K. Hashimoto, and T. Omori, "Highly piezoelectric boundary waves in $\text{Si}/\text{SiO}_2/\text{LiNbO}_3$ structure," in *Proc. IEEE Int. Freq. Contr. Symp.*, 1998, pp. 484–488.
- [13] K. Blötekjær, K. A. Ingebrigtsen, and H. Skeie, "A method for analysing waves in structures consisting of metal strips on dispersive media," *IEEE Trans. Electron. Devices*, vol. 20, no. 6, pp. 1133–1138, 1973.
- [14] K. Blötekjær, K. A. Ingebrigtsen, and H. Skeie, "Acoustic surface waves with periodic metal strips on the surface," *IEEE Trans. Electron. Devices*, vol. 20, no. 6, pp. 1139–1146, 1973.
- [15] J. J. Campbell and W. R. Jones, "A method for estimating optimal crystal cuts and propagation direction for excitation of piezoelectric surface waves," *IEEE Trans. Sonics Ultrason.*, vol. 15, no. 4, pp. 209–217, 1968.
- [16] A. H. Fahmy and E. L. Adler, "Propagation of surface acoustic waves in multilayers: A matrix description," *Appl. Phys. Lett.*, vol. 22, no. 10, pp. 495–497, 1973.
- [17] E. L. Adler, "Matrix methods applied to acoustic waves in multilayers," *IEEE Trans. Ultrason., Ferroelect., Freq. Contr.*, vol. 37, no. 6, pp. 485–490, 1990.
- [18] K. A. Ingebrigtsen, "Surface waves in piezoelectrics," *J. Appl. Phys.*, vol. 40, pp. 2681–2687, Jun. 1969.
- [19] Y. Zhang, J. Desbois, and L. Boyer, "Characteristic parameters of surface acoustic waves in a periodic metal grating on a piezoelectric substrate," *IEEE Trans. Ultrason., Ferroelect., Freq. Contr.*, vol. 40, no. 3, pp. 183–192, 1993.
- [20] E. L. Adler, "SAW and pseudo-SAW properties using matrix methods," *IEEE Trans. Ultrason., Ferroelect., Freq. Contr.*, vol. 41, no. 6, pp. 876–882, 1994.
- [21] H. P. Reichinger and A. R. Baghai-Wadji, "Dynamic 2D analysis of SAW devices including mass-loading," in *Proc. IEEE Ultrason. Symp.*, 1992, pp. 263–266.
- [22] P. Ventura, J. Desbois, and L. Boyer, "A mixed FEM/analytical model of the electrode mechanical perturbation for SAW and PSAW propagation," in *Proc. IEEE Ultrason. Symp.*, 1993, pp. 205–208.
- [23] G. Endoh, K. Hashimoto, and M. Yamaguchi, "Surface acoustic wave propagation characterization by finite element method and spectral domain analysis," *Jpn. J. Appl. Phys.*, vol. 34, no. 5B, pp. 2638–2641, 1995.
- [24] P. Ventura, J.-M. Hodé, J. Desbois, and M. Solal, "Combined FEM and green's function analysis of periodic SAW structure, application to the calculation of reflection and scattering parameters," *IEEE Trans. Ultrason., Ferroelect., Freq. Contr.*, vol. 48, no. 5, pp. 1259–1274, 2001.
- [25] P. Ventura, J.-M. Hodé, M. Solal, J. Desbois, and J. Ribbe, "Numerical methods for SAW propagation characterization," in *Proc. IEEE Ultrason. Symp.*, 1998, pp. 175–186.
- [26] K. Hashimoto, J. Koskela, and M. M. Salomaa, "Fast determination of coupling of modes parameters based on strip admittance approach," in *Proc. IEEE Ultrason. Symp.*, 1999, pp. 93–96.



Serge Camou was born in 1973 in Poissy, France. He received the DEA degree in Physical Acoustics from the Université de Paris VI–VII and then joined the Laboratoire de Physique et Métrologie des Oscillateurs (LPMO), Besançon, France, as a Ph.D. student in 1996. His thesis dissertation was dedicated to the study of acoustic wave properties in stratified structures, with applications in the field of high frequency filters. In 1998, he temporarily joined the research division of Thales Microsonics, Sophia-Antipolis, France,

for one year in the frame of his military service, where he was employed as a research engineer. He defended his thesis in 2001 and then joined the Laboratory of Integrated Micro-Mechatronics System (LIMMS/CNRS-IIS, University of Tokyo, Japan) as a postdoctoral researcher. His current interests are in developing tools to perform on-chip fluorescent spectroscopy, such as PDMS 2D optical lenses or Organic Light Emitting Devices, with applications in the field of DNA integrated detection system (lab-on-a-chip device).



Vincent Laude (M'00) was born in Bourglain-Reine, France, in 1968. He received an Engineering Diploma in 1990 from the Ecole Supérieure d'Optique and a Ph.D. in Physics in 1994 from Paris XI University, both in Orsay, France.

From 1995 to 1999, he was a researcher at Thomson-CSF (now Thales) Corporate Research Laboratory in Orsay, France, where he worked on various aspects of optical signal processing, wavefront sensing, and ultrashort laser pulses. In 2000, he joined Thomson-CSF

Microsonics in Sophia-Antipolis, France, to work on surface acoustic wave propagation. At the end of the same year, he joined the Laboratoire de Physique et Métrologie des Oscillateurs, Centre National de la Recherche Scientifique in Besançon, France. He is currently

interested in the propagation of surface and guided acoustic waves and their interactions with microstructures.

Vincent Laude is a member of IEEE/UFFC.



Thomas Pastureaud was born in Blaye, France, in 1976. He received an Engineering Diploma in 1998 from the Ecole Supérieure de Physique et de Chimie Industrielle de Paris, and a DEA (master) degree in Physical Acoustics from Université Paris VII. He joined the Laboratoire de Physique et Métrologie des Oscillateurs, Centre National de la Recherche Scientifique in Besançon, France, as a doctorate student in 1999. He is also with Thales Microsonics, Sophia Antipolis, France. He has been working in the field of surface acoustic

waves and is especially interested in the analysis of new structures and propagation mechanisms.

Sylvain Ballandras was born in Strasbourg, France. He received the DEA degree in Acousto-Opto-Electronique et Vibrations and the Ph.D. degree in Science Pour l'Ingénieur from the Université de Franche-Comté, Besançon, France.

He joined the Laboratoire de Physique et Métrologie des Oscillateurs (LPMO), Besançon, France, staff member in 1991. He has been working in the fields of SAW sensitivity to physical perturbations and in parallel in microtechnologies, such as LIGA and Stereolithography. He received the Habilitation à Diriger des Recherches degree from the Université de Franche-Comté in 1997. He joined Thomson Microsonics for one year as a research engineer. He went back to the LPMO in 1998. Since 1999, he has been heading the Acoustics and Microsonics research group at the LPMO. His current interests are in the application of SAW devices (sensors) in the development of numerical models and new technologies for ultrasound transducers devoted to acoustic imaging and nondestructive control.